

# Hole-enhanced electron injection from ZnO in inverted polymer light-emitting diodes

Lu, Mingtao; de Bruyn, Paul; Nicolai, Herman T.; Wetzelaer, Gert-Jan A. H.; Blom, Paul W. M.

*Published in:*
Organic Electronics

*DOI:*
10.1016/j.orgel.2012.05.032



*Publication date:*
2012

Organic Electronics 13 (2012) 1693–1699

Contents lists available at SciVerse ScienceDirect

Organic Electronics

journal homepage: www.elsevier.com/locate/orgel

# Hole-enhanced electron injection from ZnO in inverted polymer light-emitting diodes

Mingtao Lu [a,b,*], Paul de Bruyn [a,b], Herman T. Nicolai [a], Gert-Jan A.H. Wetzelaer [a,b], Paul W.M. Blom [a,c]

[a] Molecular Electronics, Zernike Institute for Advanced Materials, University of Groningen, Nijenborgh 4, 9747 AG Groningen, The Netherlands
[b] Dutch Polymer Institute, P.O. Box 902, 5600 AX Eindhoven, The Netherlands
[c] TNO/Holst Centre, High Tech Campus 31, 5605 KN Eindhoven, The Netherlands

ARTICLE INFO

*Article history:*
Received 6 February 2012
Received in revised form 14 May 2012
Accepted 17 May 2012
Available online 30 May 2012

*Keywords:*
Polymer
Light-emitting diode
Zinc oxide
Inverted
Injection barrier
Organic

ABSTRACT

Metal oxides as ZnO provide an interesting alternative for conventional low work function metals as electron injection layer in organic light-emitting diodes (OLEDs). However, for most state-of-the-art OLED materials the high work function of ZnO leads to a large injection barrier for electrons. As a result the electron current in the OLED is largely limited by the contact, leading to a strong reduction of the conversion efficiency. Here we demonstrate that by depositing an amorphous ZnO layer as cathode in an inverted polymer LED, the electron injection can be strongly enhanced by electrical conditioning. For suited polymers comparable conversion efficiencies of the conventional and inverted PLEDs can be achieved.



## 1. Introduction

The concept of organic light-emitting diodes (OLEDs) dates back to 1987, when Tang et al. fabricated the first OLED with Tris(8-hydroxyquinolinato)aluminium ($Alq_3$) as the active layer [1]. In the following two decades, more and more organic compounds were adopted for lighting applications. To achieve an Ohmic contact for electron injection, low work-function metals, such as Ca or Ba, are commonly used as cathodes in OLEDs. However, these metals are not stable toward air and moisture, requiring rigorous encapsulation. Furthermore, they must be deposited under high vacuum. Since low cost and flexibility are major assets of OLEDs, the focus in research has recently shifted toward solution-processed OLEDs. Solution-processable metal oxides, such as MgO, $TiO_2$ or ZnO, are particularly suitable for these applications, as evidenced by reports on polymer light-emitting diodes (PLEDs) with inverted structures [2,3]. Note that although $TiO_2$ and ZnO are far more air-stable as compared to standard Ba/Al cathodes, they are still sensitive to the oxygen in the air. However, through thermal annealing or under UV radiation, the absorbed oxygen on $TiO_2$ or ZnO surface can be released and the fabricated PLEDs can be recovered [4]. Because of its conductivity, suitable energy levels and transparency, ZnO has been widely used as electron-extracting contact in organic photovoltaics (OPVs) [5–7]. The ZnO we use has a work function of 4.2 eV [6], as measured with a Kelvin probe (for more details see Section 2). This work function aligns well with the lowest unoccupied molecular orbitals (LUMOs) of fullerene acceptor materials used in OPVs. Note that the work function of ZnO varies with deposition/processing conditions. Through a low temperature annealing process described in this paper, a ZnO thin film with a work function of 4.2 eV is achieved. However, most

* Corresponding author at: Molecular Electronics, Zernike Institute for Advanced Materials, University of Groningen, Nijenborgh 4, 9747 AG Groningen, The Netherlands.
*E-mail address:* M.Lu@rug.nl (M. Lu).

1566-1199/$ - see front matter © 2012 Elsevier B.V. All rights reserved.
http://dx.doi.org/10.1016/j.orgel.2012.05.032

state-of-the-art light-emitting small molecules and polymers, such as poly(*p*-phenylene vinylene) (PPV) or polyfluorene (PFO) derivatives, have their LUMO around 2.9 eV below the vacuum level. When applying ZnO as the cathode in a PLED structure, the mismatch between the work function of ZnO and the LUMO of the light-emitting polymer (LEP) gives rise to a large injection barrier for electrons. The resulting unbalanced electron- and hole-transport then leads to a strong reduction of the PLED efficiency. Many approaches have been employed to reduce this injection barrier, such as deposition of a layer of $Cs_2CO_3$ between ZnO and the polymer [8–10], blending an ionic liquid in the polymer solution, resulting in light-emitting electrochemical cells [11], or growing a self-assembled monolayer on the ZnO surface [12,13]. It has been reported that without these modifications the inverted PLEDs do not generate light at all, as a result of insufficient electron injection.

To investigate the influence of the electron injection barrier on device performance, we fabricated PLEDs with both conventional and inverted structures. Here we demonstrate that by using a low temperature annealing process, the deposited amorphous ZnO layer acts as hole blocking layer and the PLED device can be switched on by the electrical conditioning.

## 2. Experimental

Poly(2-methoxy-5-(2′-ethyl-hexyloxy)-*p*-phenylene vinylene) (MEH-PPV) was synthesized as described previously [14]. Poly[9,9-didecanefluorene-alt-(*bis*-thienylene)benzothiadiazole] (PF10TBT) and an indacenodithiophene copolymer with a benzothiadiazole acceptor unit (IDT-BT) were obtained from TNO and Imperial College, respectively, and used as received.

To fabricate an inverted PLED, a layer of ZnO was deposited on an ITO substrate as the bottom cathode. Zinc acetyl acetonate hydrate [$Zn(acac)_2$] was used as a precursor, which was purchased from Sigma–Aldrich and used without further purification. $Zn(acac)_2$ was dissolved in ethanol and kept at 50 °C. ITO substrates were heated at the same temperature. After spin coating, the $Zn(acac)_2$ layer was annealed at 120 °C in ambient condition. The $Zn(acac)_2$ precursor hydrolyzed and formed a thin layer of ZnO (20 nm) [15]. The work function of the ZnO layer was measured with a Kelvin probe in nitrogen atmosphere relative to a gold reference, which was calibrated under nitrogen atmosphere against highly oriented pyrolytic graphite (HOPG). A 70 nm MEH-PPV layer, a 55 nm PF10TBT layer and a 55 nm IDT-BT layer were spin casted respectively as the active layer. The device is encapsulated by evaporating a 10 nm $MoO_3$ layer and a 100 nm Al layer in a vacuum chamber under a base pressure of $1 \times 10^{-7}$ mBar. PLEDs with a conventional structure were fabricated with polymers sandwiched between a poly(3,4-ethylenedioxythiophene):poly(4-styrene sulfonate) (PEDOT:PSS) covered ITO anode, and a Al (100 nm) covered Ba (5 nm) cathode. The *J–V* characteristics were recorded by using a Keithley 2400 source meter. The generated light was collected by a Si-photodiode connected to a Keithley 6514 electrometer. The impedance spectroscopy was measured by using an Agilent 4284A precision LCR meter. All the measurements were carried out in a nitrogen atmosphere.

## 3. Results and discussion

Fig. 1a shows the *J–V* and *L–V* characteristics of the conventional and inverted PLEDs based on MEH-PPV. The *J–V* characteristics of a conventional PLED can be divided in three regimes: (1) the leakage–current regime, where the relation between current and voltage obeys Ohm's law; (2) the diffusion-dominated current regime, where the current depends exponentially on the applied voltage, appearing as a straight line on a semilogarithmic plot; (3) the drift current dominating regime, where the current depends quadratically on voltage [16]. At the built-in voltage ($V_{bi}$), a transition from the diffusion-dominated to the drift-dominated regime occurs, indicated by the point at which the device current starts to deviate from the line in Fig. 1a. For Ohmic electron- and hole-contacts the built-in voltage is governed by the bandgap of the LEP, whereas for non-Ohmic contacts the built-in voltage is determined by the difference between the work function of the electrodes. In a conventional MEH-PPV PLED, Ohmic contacts as PEDOT:PSS anode (5.1 eV) and Ba cathode (2.9 eV) are used, leading to a $V_{bi}$ of typically 2 V. Accordingly, in the *J–V* characteristics of Fig. 1a the currents bends away from the straight line at around 2 V. It is also evident from the *J–V* characteristics that $V_{bi}$ is much smaller for an inverted PLED, which can be understood from the higher work function of ZnO compared to that of Ba. In the inverted PLED $MoO_3$ is used as the anode, which has a work function as high as 6.9 eV [17–19]. However, since the highest occupied molecular orbital (HOMO) of MEH-PPV is located around 5.3 eV, the Fermi-level of $MoO_3$ is pinned to the HOMO of the polymer. In this case, the built-in voltage of the inverted PLED is determined by the difference between the work function of ZnO and the HOMO of the polymer, which is around 1.1 eV. Consequently, the inverted PLED shows a smaller $V_{bi}$ in the *J–V* characteristics.

In Fig. 1a the diffusion current in the conventional PLED exceeds the leakage current at 1.6 V. Correspondingly, light is detected by the photodiode at the same voltage, indicating that the current is carried by both electrons and holes. The onset of the current of the inverted PLED is around 0.5 V. However, no light-output was detected at this voltage. Since the hole-injecting contact is Ohmic and a large electron-injection barrier is present in the device, the current in the MEH-PPV layer is solely conducted by holes. Note that as an n-type semiconductor, the conduction band of ZnO is close to its Fermi level (4.2 eV below the vacuum level). The band gap of ZnO is around 3.3 eV, therefore the valence band locates at around 7.5 eV below the vacuum level, which is 2.3 eV deeper than the HOMO of MEH-PPV. The large injection barrier makes hole injection from the MEH-PPV into the ZnO layer unfavorable. As a result, it is expected that the holes will recombine with the electrons at the ZnO/polymer interface. Under high bias voltage, the device current of the conventional and the inverted PLEDs are comparable since in a conventional MEH-PPV PLED the current is mainly carried by holes. The electron transport is hampered by deep traps, resulting in an electron

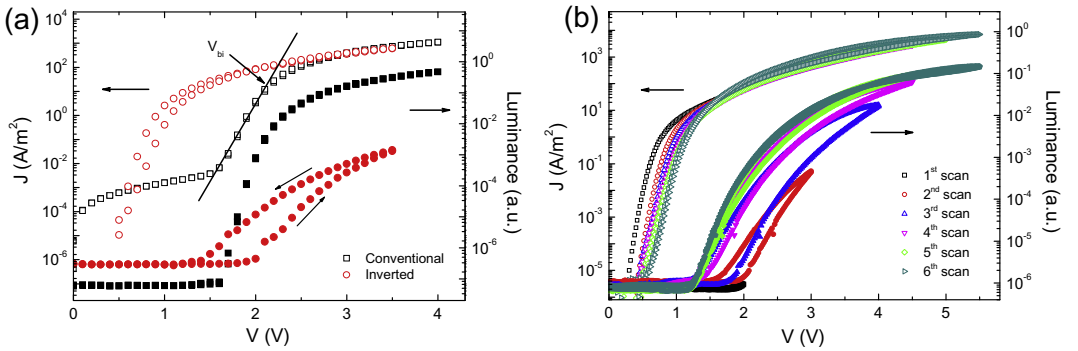


**Fig. 1.** (a) The *J–V* (open symbols) and *L–V* characteristics (solid symbols) of a conventional PLED and an inverted PLED. Both the devices have the same thickness: 90 nm. (b) Subsequent *J–V* (open symbols) and *L–V* (solid symbols) of a MEH-PPV inverted PLED.

current that is orders of magnitude lower than the hole current [20–22]. For both devices the hole injection is Ohmic and the thicknesses of the polymer layers are same. As a result, the hole current, as well as the total current, are comparable in the two devices. Furthermore, at a given voltage $V$ the effective voltage $V - V_{bi}$ across the inverted device is higher, giving rise to an enhanced current, such that the difference in electron current is indiscernible in the *J–V* characteristics. When the applied voltage is larger than 2.0 V, the inverted PLED starts to generate light and a counterclockwise hysteresis appears on the *L–V* plot. As a consequence, the light-emission can be enhanced by electrical conditioning. We postulate that the electron-injection barrier is reduced by the presence of a hole current. The holes travel across the active layer and accumulate at the ZnO/polymer interface, thereby changing the local electric field at the cathode. As the accumulated holes cause band bending, the electron-injection barrier is reduced. As a result, electron injection can be switched on by electrical conditioning. A similar switching process has been observed previously for hole injection from a PEDOT:PSS anode in polyfluorene-based devices [23,24]. Before the inverted PLED is switched on, the luminance of the conventional PLED is 4 orders of magnitude higher than that of the inverted PLED. Since light is generated by recombination of electrons and holes in the active layer and for both devices the hole contact is Ohmic, the difference in luminance can be attributed to a difference in electron injection. According to an empirical relation found by Asadi et al., the current is exponentially related to the injection barrier with a slope of 0.25 eV/decade at an electric field of 20 MV/m [25]. In an MEH-PPV inverted PLED the electron injection barrier is around 1.3 eV. As a result, the electron current, and hence luminance, should be reduced by around 5 orders of magnitude as compared to a conventional device, which is indeed observed in our measurements before switching.

To verify whether accumulated holes enhance the electron injection, we studied the light-emission improvement as a function of the maximum applied bias, as can be seen in the subsequent *J–V* measurements in Fig. 1b. As the maximum voltage of each sweep increases, an advancing hysteresis is observed, resulting in an increase of the luminance of the inverted PLED. By applying a higher voltage, more holes accumulate at the cathode–polymer interface and cause further reduction of the injection barrier. The *L–V* curve saturates at the 6th scan, which has a maximum scanning voltage of 5.5 V. This indicates that at this voltage all interface states are occupied by holes and further improvement of the device performance cannot be achieved by electrical conditioning.

Fig. 2a shows the normalized conversion efficiency (CE) as a function of the applied bias voltage after electrical

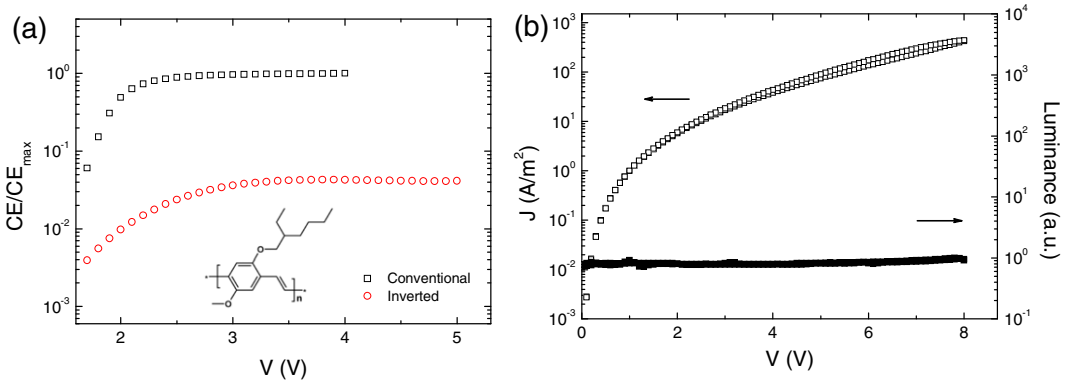


**Fig. 2.** (a) Conversion efficiencies of a conventional PLED and a fully switched-on inverted PLED. All the devices have the same thickness: 90 nm. The inset shows the chemical structure of MEH-PPV. (b) *J–V* (open symbols) and *L–V* (solid symbols) characteristics of a MEH-PPV inverted PLED. The device was annealed at 300 °C for 20 min. The device thickness is 170 nm.

conditioning. Although the device performance is largely improved by electrical conditioning, the efficiency of the inverted PLED is still more than one order of magnitude lower than that of the conventional device, indicating that a small injection barrier of about 0.3–0.4 eV is still present.

The observation of efficient injection from a relatively high work function material such as ZnO is not straightforward. In Refs. [26,27] inverted PLEDs were made with "super yellow" and an aryl-polyfluorene homopolymer as active layers, respectively. The LUMOs of these two polymers are comparable to that of MEH-PPV. However, the fabricated inverted PLEDs did not generate light and a thin layer of $Cs_2CO_3$ was required to improve the electron injection. In contrast, our inverted PLEDs can be switched on by electrical conditioning, even without a $Cs_2CO_3$ layer. This can be attributed to the different deposition procedure of the ZnO layer. In the studies described in Refs. [26,27], the ZnO layer is deposited through spray pyrolysis from a zinc acetate dihydrate precursor and subsequently annealed at 400–500 °C. As Zn interstitials, oxygen vacancies and hydrogen complexes are native defects in undoped bulk ZnO, the high-temperature annealing process reduces the concentration of defects [28]. Therefore, the ZnO layer is more compact and highly crystalline [29]. In our case, the ZnO layer was spin cast in air from a $Zn(acac)_2$ precursor solution and annealed at a rather low temperature (120 °C) and is therefore amorphous [12]. The defects on the surface of the ZnO layer may provide empty states for holes. As holes are trapped at the ZnO/polymer interface, they induce an electric field and cause a shift of the vacuum level. As a result, an electroforming effect is observed. To further investigate the role of defects we show in Fig. 2b the *J–L–V* characteristics of a MEH-PPV inverted PLED, of which the ZnO layer is annealed at 300 °C for 20 min. Although the device current is very high, no light output or switching effect was observed. This can be explained by a reduction of the defect states at the ZnO/MEH-PPV interface, that eliminates the hole trapping.

It is relevant to know to what extent the electron injection barrier can be surmounted by electrical conditioning in other material systems. Therefore, we deliberately varied the injection barrier by choosing LEPs with different LUMOs. Here, we fabricated conventional and inverted PLEDs with PF10TBT and IDT-BT as the active layers. The LUMO of PF10TBT is 3.4 eV [30], which reduces the electron injection barrier in an inverted PLED to 0.8 eV. The LUMO of IDT-BT is located at 3.6 eV, obtained by adding the optical band gap to the experimentally determined HOMO [31,32]. Similar to the MEH-PPV inverted PLEDs, counterclockwise hysteresis appears on the first sweep of the *L–V* characteristics for both polymers (Fig. 3a and c). After the inverted PLEDs were switched on by electrical conditioning, the luminance and the conversion efficiencies of the conventional and inverted PLEDs are comparable (Fig. 3a–c), which is attributed to a smaller injection barrier for electrons. According to the 0.25 eV per decade

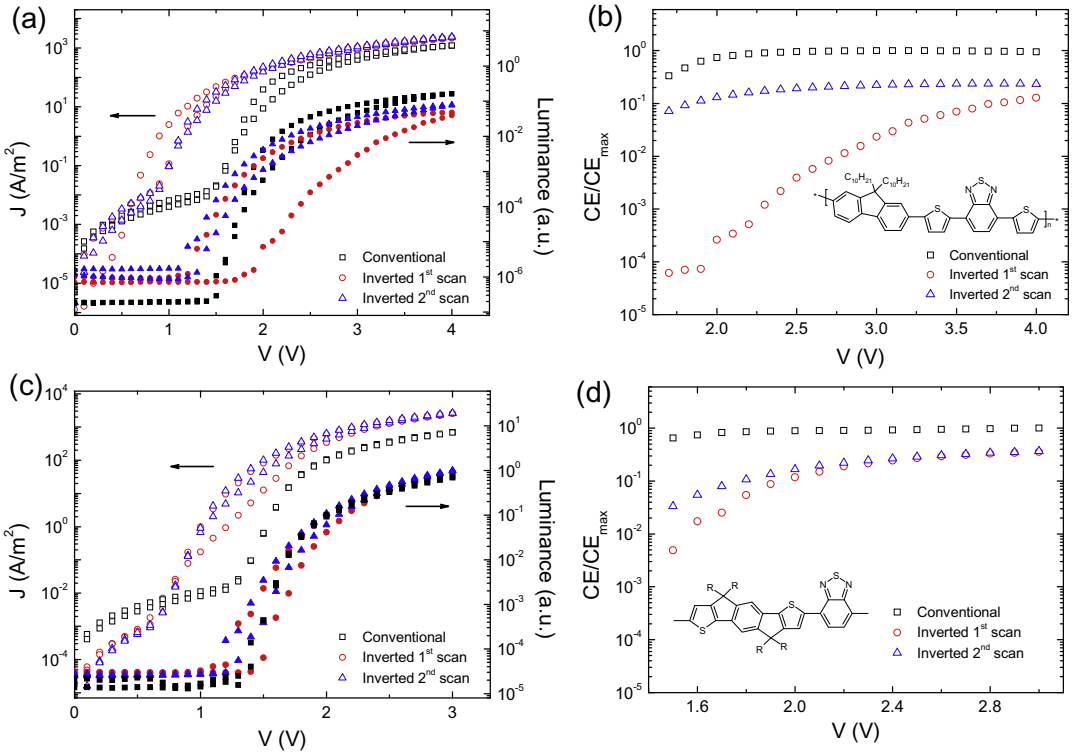


**Fig. 3.** *J–V* (open symbols) and *L–V* (solid symbols) characteristics of (a) PF10TBT and (c) IDT-BT conventional and inverted PLEDs. All the devices have the same thickness: 55 nm. The conversion efficiencies of the same devices are shown in (b) (PF10TBT) and (d) (IDT-BT). The chemical structures of PF10TBT and IDT-BT are shown in insets of (b) and (d), respectively.

**Table 1**
The modulation of the conversion efficiency of an inverted PLED by the injection barrier.

| | Injection barrier (eV) | QE inverted/QE conventional (%) |
|---|---|---|
| IDT-BT | 0.6 | 36.8 |
| PF10TBT | 0.8 | 23.6 |
| MEH-PPV | 1.3 | 4.3 |

current modulation rule [25], the electron current in these two devices should be reduced by a factor of 1500 (for PF10TBT) and 250 (for IDT-BT), respectively. Indeed, the difference between the luminance of conventional and inverted PLEDs before electrical conditioning amounts to 2 (for PF10TBT) and 1 (for IDT-BT) orders of magnitude, respectively. The modulation of the conversion efficiency after electrical conditioning is summarized in Table 1. For injection barriers of 0.6 eV and 0.8 eV the CE of the inverted device is close to the CE of the conventional device, indicating that barriers of up to 0.8 eV can indeed be overcome by the electrical forming process. Furthermore, we observe from Fig. 3 that the light-output of the inverted device after electrical forming is equal to the light-output of the conventional device as a function of voltage. However, due to the enhanced effective voltage $V - V_{bi}$ the current in the inverted device is higher, leading to a slightly reduced efficiency.

An effective way to study the accumulation of holes at the ZnO/polymer interface is impedance spectroscopy (IS). An AC voltage of 0.01 V is superimposed on a DC voltage that is applied to the device. The frequency of the AC voltage was swept from 20 Hz to 1 MHz and the DC voltage was scanned from 0 to 4 V. Fig. 4 shows the real and imaginary parts of the impedance of a PF10TBT inverted PLED as an example. At an applied DC voltage of 1.0 V, one semicircle appeared in the Nyquist-plot (Fig. 4a). The semicircle was modeled with an equivalent single RC circuit (Fig. 4a inset), enabling the determination of the series resistance ($R_s$), estimated at approximately 136 Ohm. The series resistance is attributed to the resistance of ITO/ZnO. Note that in a conventional PLED, the series resistance, *viz.* the resistance of the ITO/PEDOT:PSS layers, is much smaller (around 30 Ω). The geometrical capacitance ($C_g$), which stems from the two flat electrodes, is approximately 6 nF. With a device area of $1.58 \times 10^{-5}$ m$^{-2}$, a layer thickness of 55 nm, and a polymer dielectric constant of 2.4, the geometrical capacitance is calculated to be 6.1 nF, which is in agreement with the value deduced from the impedance measurements. At a DC voltage of 1.4 V, the device was switched on by electrical conditioning and two semi-circles appear in the Nyquist-plot (Fig. 4b). The curve can be modeled with an equivalent double RC circuit (Fig. 4b inset). The second capacitance ($C_i$), which is approximately 302 nF, is attributed to hole accumulation at the ZnO/polymer interface. Fig. 5a shows the differential capacitances $C_g$ and $C_i$ as a function of the DC voltage. As expected, $C_g$ does not depend on the applied bias voltage. However, during the up-scan of the DC voltage sweep, a decrease of $C_i$ is observed. This might be caused by the fact that due to the increased electron injection during the forming process part of the holes accumulated at the ZnO/polymer interface are released by recombinations with the additional electrons injected from the ZnO contact. Since part of the holes were "permanently" trapped at the interface, *viz.* the escape time is much longer than the time period of the *J–V* sweeps, the capacitance of the interface is reduced (Fig. 5a). As a result, $C_i$ during the down-scan is smaller than that during the up-scan. These "permanently" trapped holes are then responsible for the forming effect. With the interface capacity known we can also calculate the amount of accumulated holes $N_i$ at the ZnO/polymer interface from Eq. (1)

$$N_i = \frac{1}{eA}\int_0^V C_i dV, \tag{1}$$

Fig. 5b shows that $N_i$ is invariant under different DC voltages, indicating that $N_i$ saturates at approximately $4.5 \times 10^{16}$ m$^{-2}$. Using Gauss's law (Eq. (2)), the change of the electric field resulting from the positive charges on the interface can be calculated as $8 \times 10^8$ V/m.

$$\oint \vec{E} \cdot d\vec{S} = \frac{Q_f + Q_P}{\varepsilon_0} \tag{2}$$

where $Q_f$ is the free charge and $Q_p$ is the bound charge. The positive charges induce charge dipoles and result in a shift

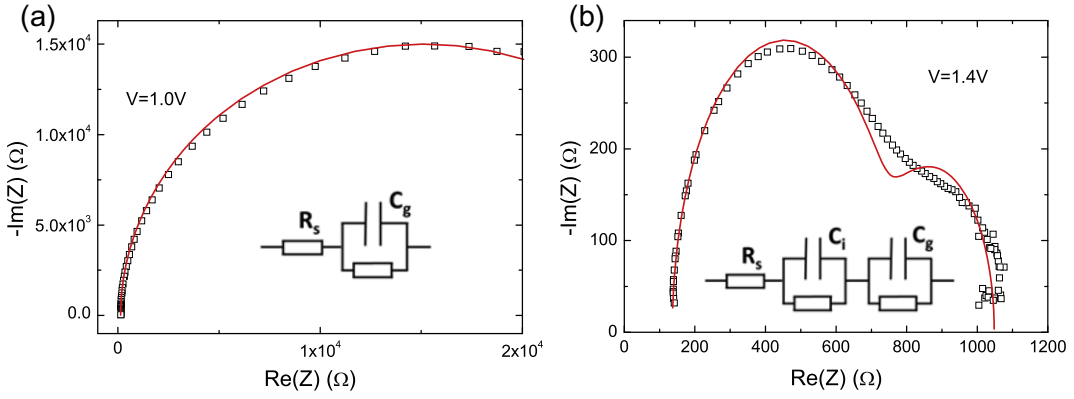


**Fig. 4.** Impedance spectroscopy of a PF10TBT inverted PLED. The applied DC bias voltages are (a) 1.0 V and (b) 1.4 V. The insets of (a) and (b) shows the equivalent RC circuits. The solid lines represent the calculations from the equivalent circuits.

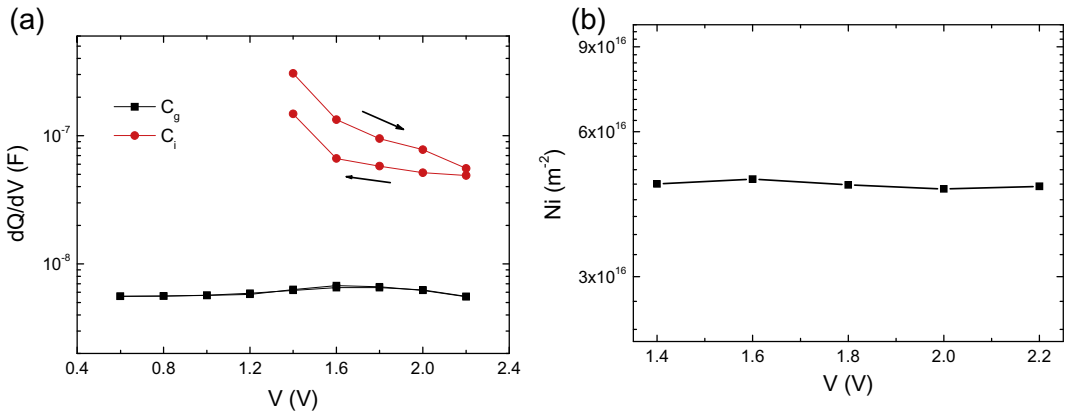


**Fig. 5.** (a) The differential capacitances $C_g$ and $C_i$ as a function of the applied bias voltage. (b) The density of holes on the ZnO/PF10TBT interface at different voltages.

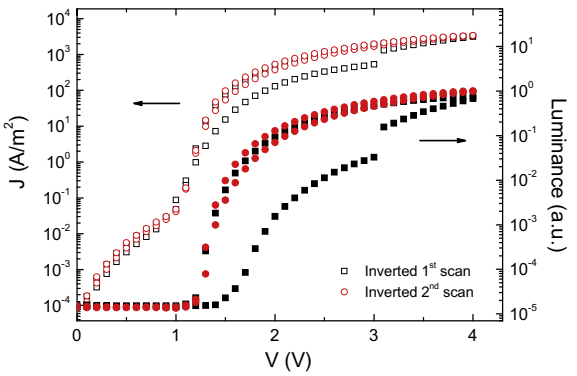


**Fig. 6.** *J–V* (open symbols) and *L–V* (solid symbols) characteristics of a PF10TBT inverted PLED, which was previously switched on and measured again after being kept in a nitrogen atmosphere for twelve hours. The device thickness is 55 nm.

of the vacuum level [33,34]. Assuming the thickness of the interfacial layer to be 1 nm, the shift of the vacuum level would be around 0.8 eV. This value is in agreement with the electron injection barrier in the PF10TBT inverted device, which confirms that a barrier of 0.8 eV can indeed be overcome with $4.5 \times 10^{16}\,m^{-2}$ trapped holes at the ZnO/polymer interface. In a nitrogen atmosphere, without thermal or photo activation, the trapped holes on the polymer/ZnO interface will be released after one day (Fig. 6).

## 4. Conclusion

We have fabricated inverted PLEDs with non-reactive metal oxides as the electrodes. The work function of ZnO is higher than the LUMO of most light-emitting materials, resulting in an electron-injection barrier for the inverted PLEDs. As the deposited amorphous ZnO layer contains a large concentration of defects, it may provide surface states for holes. With holes accumulating on the ZnO/polymer interface, the device can be switched on by electrical conditioning. For inverted PLEDs with a smaller electron injection barrier, the device performances of the conventional and inverted devices are comparable. Here we demonstrate that electron injection barriers up to 0.8 eV can be largely surmounted by electrical conditioning.

## Acknowledgements

This work is part of the Dutch Polymer Institute research program (Project #618). The authors would like to thank Jan Harkema and Frans van der Horst for technical support, and Jurjen Wildeman for synthesizing MEH-PPV. Prof. Iain McCulloch and Dr. Martin Heeney (Imperial College) and Jörgen Sweelssen (TNO) are acknowledged for supplying IDT-BT and PF10TBT, respectively.

## Reference

[1] C.W. Tang, S.A. VanSlyke, Appl. Phys. Lett. 51 (1987) 913.
[2] H.J. Bolink, H. Brine, E. Coronado, M. Sessolo, J. Mater. Chem. 20 (2010) 4047.
[3] H.J. Bolink, E. Coronado, D. Repetto, M. Sessolo, Appl. Phys. Lett. 91 (2007) 223501.
[4] F. Verbakel, S.C. Meskers, R.A. Janssen, Appl. Phys. Lett. 89 (2006) 102103.
[5] D.J.D. Moet, P. de Bruyn, P.W.M. Blom, Appl. Phys. Lett. 96 (2010) 153504.
[6] P. de Bruyn, D.J.D. Moet, P.W.M. Blom, Org. Electron. 11 (2010) 1419.
[7] Y. Sun, J.H. Seo, C.J. Takacs, J. Seifter, A.J. Heeger, Adv. Mater. 23 (2011) 1679.
[8] Y. Vaynzof, D. Kabra, L.L. Chua, R.H. Friend, Appl. Phys. Lett. 98 (2011) 113306.
[9] D. Kabra, L.P. Lu, M.H. Song, H.J. Snaith, R.H. Friend, Adv. Mater. 22 (2010) 3194.
[10] T. Lee, J. Hwang, S. Min, Chem. Sus. Chem. 3 (2010) 1021.
[11] H.J. Lee, B.R. Lee, J.S. Park, S.O. Kim, J.Y. Kim, M.H. Song, Appl. Phys. Lett. 98 (2011) 253309.
[12] C.-Y. Li, Y.-N. Chou, J.-R. Syu, S.-N. Hsieh, T.-D. Tsai, C.-H. Wu, T.-F. Guo, W.-C. Hsu, Y.-J. Hsu, T.-C. Wen, Org. Electron. 12 (2011) 1477.
[13] J.S. Park, B.R. Lee, J.M. Lee, J.-S. Kim, S.O. Kim, M.H. Song, Appl. Phys. Lett. 96 (2010) 243306.
[14] C. Tanase, J. Wildeman, P.W.M. Blom, Adv. Funct. Mater. 15 (2005) 2011.
[15] T. Arii, A. Kishi, J. Therm. Anal. Calorim. 83 (2006) 253.
[16] K. Weiser, Science 170 (1970) 966.
[17] M. Kröger, S. Hamwi, J. Meyer, T. Riedl, W. Kowalsky, A. Kahn, Org. Electron. 10 (2009) 932.
[18] J. Meyer, A. Shu, M. Kroger, A. Kahn, Appl. Phys. Lett. 96 (2010) 133308.
[19] M. Kroger, H. Hamwi, T. Riedl, W. Kowalsky, A. Kahn, Appl. Phys. Lett. 95 (2009) 123301.
[20] P.W.M. Blom, M.J.M. de Jong, J.J.M. Vleggaar, Appl. Phys. Lett. 68 (1996) 3308.

[21] H. Antoniadis, M.A. Abkowitz, B.R. Hsieh, Appl. Phys. Lett. 65 (1994) 2030.
[22] M.M. Mandoc, B. de Boer, G. Paasch, P.W.M. Blom, Phys. Rev. B 75 (2007) 193202.
[23] T. van Woudenbergh, J. Wildeman, P.W.M. Blom, J.J.A.M. Bastiaansen, B.M.W. Langeveld-Vos, Adv. Funct. Mater. 14 (2004) 677.
[24] D. Poplavskyy, J. Nelson, D.D.C. Bradley, Appl. Phys. Lett. 83 (2003) 707.
[25] K. Asadi, T.G. de Boer, P.W.M. Blom, D.M. de Leeuw, Adv. Funct. Mater. 19 (2009) 3173.
[26] H.J. Bolink, E. Coronado, J. Orozco, M. Sessolo, Adv. Mater. 21 (2009) 79.
[27] L. Lu, D. Kabra, K. Johnson, R.H. Friend, Adv. Funct. Mater. 22 (2012) 144.
[28] S.J. Pearton, D.P. Norton, K. Ip, Y.W. Heo, T. Steiner, J. Vac. Sci. Technol. B 22 (2004) 932.
[29] T.P. Alexander, T.J. Bukowski, D.R. Uhlmann, G. Teowee, K.C. McCarthy, J. Dawley, B.J. Zelinski, Proc. 10th Int. Symp. Applicat. Ferroelect. 2 (1996) 585.
[30] D.J.D. Moet, M. Lenes, J.D. Kotlarski, S.C. Veenstra, J. Sweelssen, M.M. Koetse, B. de Boer, P.W.M. Blom, Org. Electron. 10 (2009) 1275.
[31] W. Zhang, J. Smith, S.E. Watkins, R. Gysel, M. McGehee, A. Salleo, J. Kirkpatrick, S. Ashraf, T. Anthopoulos, M. Heeney, I. McCulloch, J. Am. Chem. Soc. 132 (2010) 11437.
[32] J. Kirkpatrick, C.B. Nielsen, W. Zhang, H. Bronstein, R.S. Ashraf, M. Heeney, I. McCulloch, Adv. Energy Mater. 2 (2012) 260.
[33] I.G. Hill, A. Rajagopal, A. Kahn, Y. Hu, Appl. Phys. Lett. 73 (1998) 662.
[34] H. Ishii, K. Sugiyama, E. Ito, K. Seki, Adv. Mater. 11 (1999) 605.